More information on flow properties and handling of powders and bulk solids can be found in:

Powders and Bulk Solids
– Behavior, Characterization, Storage and Flow

by Dietmar Schulze

2nd ed. 2021, published by Springer
(Link: https://www.springer.com/us/book/9783030767198)

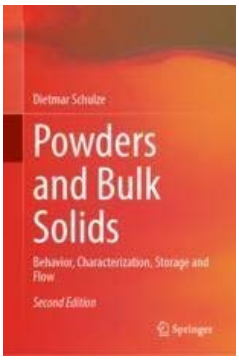

Stresses in Silos

Dietmar Schulze[1]

In containers filled with powders or bulk solids, such as silos, hoppers and IBCs, stresses occur due to gravity. These stresses cannot be calculated analogously to the pressure in a liquid. Above all, the property of bulk solids to transmit friction even at rest results in a completely different behavior.

1 Introduction

Knowledge of the stresses acting in silos and other types of containers filled with powders or bulk solids is important for many applications:

- Silo design for flow
- Structural silo design
- Loads on feeders and inserts
- Driving forces of feeders
- Design of silos in which a certain maximum stress is not exceeded (e.g. to avoid silo quaking, product destruction or extreme time consolidation)

In the following, some simple calculation equations and the required bulk solid properties are explained. Depending on the application, however, additional effects and safety factors must be taken into account. For example, for structural silo design, the approach and parameters are selected in such a way that a higher load on the silo structure tends to result from the calculation.

2 Stresses in bulk solid

For stress calculations in bulk solids technology, bulk solids are usually considered as a continuum, not as individual particles. Therefore, continuum mechanical approaches are applied.

[1] Prof. Dr. Dietmar Schulze, Dr. Dietmar Schulze GmbH, Wolfenbüttel, Germany.
E-Mail: mail@dietmar-schulze.de, Internet: www.dietmar-schulze.de

Fig. 1 shows a cylinder filled with bulk solid (frictionless walls, gravity neglected). In the vertical direction, the vertical stress, σ_v, is exerted through a piston and acts on the bulk solid. Due to the vertical stress, σ_v, the stress σ_h is acting in the horizontal direction. The ratio of the stresses, σ_v and σ_h, is called the lateral (or horizontal) stress ratio, K (also known as λ):

$$K = \frac{\sigma_h}{\sigma_v} \tag{1}$$

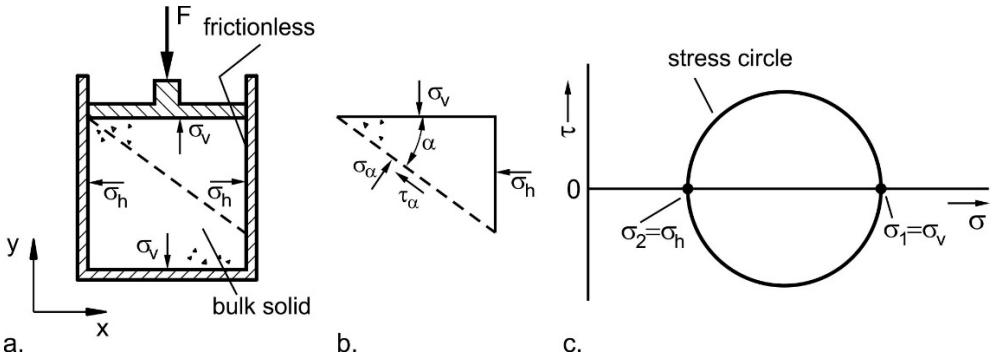

Fig. 1: a. Cylinder filled with bulk solid; b. element of bulk solid; c. Mohr stress circle

The value of the stress ratio differs with the bulk solid. While an perfectly rigid, inelastic solid body would have a stress ratio $K = 0$, and a Newtonian fluid at rest $K = 1$, the usual values for bulk solids (e.g. in silos) are usually in the range of 0.3 to 0.6, in rare cases also beyond these limits [1-3].

Not only the horizontal and vertical stresses are different, but also in inclined sectional planes (e.g. dashed line in Fig. 1a) different normal stresses, σ, but also shear stresses, τ, act. These normal and shear stresses acting in differently inclined sectional planes of a bulk solid element can be calculated by setting up force equilibrium on this bulk solid element (Fig. 1b) to calculate the stresses, σ_α and τ_α, in the sectional plane inclined by an angle α (more on this in [1, 4]).

If the pairs of values (σ_α, τ_α) for all possible angles, α, are plotted in a normal stress - shear stress diagram, they form a circle, the so-called Mohr stress circle (Fig. 1c). Each point of the stress circle gives the stresses in a cutting plane. In each case, one can find a cutting plane in which the normal stress acting there is greatest. This plane is represented by the right intersection of the stress circle with the normal stress axis. In the case of the model test of Fig. 1a, this is the horizontal plane in which the vertical stress, σ_v, is acting. This largest normal stress is called the major principal stress, σ_1. Exactly perpendicular to σ_1 acts the smallest of the normal stresses acting in the different sections, the minor principal stress, σ_2. This stress corresponds to the horizontal stress σ_h in the case of Fig. 1 [1, 4].

3 Stresses in silos, bins and hoppers

In contrast to a liquid, a bulk solid can transmit shear stresses even when at rest. While the pressure in a liquid container increases linearly with depth (Fig. 2), in a cylindrical bulk solid container of constant cross-section the shear stress exerted by the bulk solid on the container wall – the friction on the container wall – carries a part of the weight of the bulk solid column. As a result, the vertical stress increases less compared to the pressure in the liquid. With sufficient depth the vertical stress becomes constant.

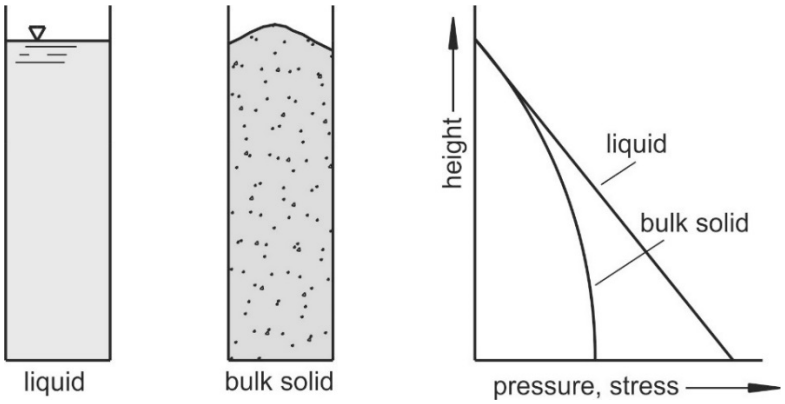

Fig. 2: Pressure in a liquid and stress in a bulk solid (in principle)

If an empty silo is filled, a stress curve as shown in Fig. 3a [5] results. The wall normal stress, σ_w, increases downward in the vertical section to finally approach a final value asymptotically (as already shown in Fig. 2). In the vertical section, the vertical stresses are the larger stresses, while the (smaller) horizontal stresses occur according to the stress ratio, K, given by Eq. (1). The major principal stress, σ_1, points in the axis in the vertical direction. Towards the walls, the major principal stress increasingly deviates from the vertical because of the effect of wall friction (see principal stress lines in Fig. 3).

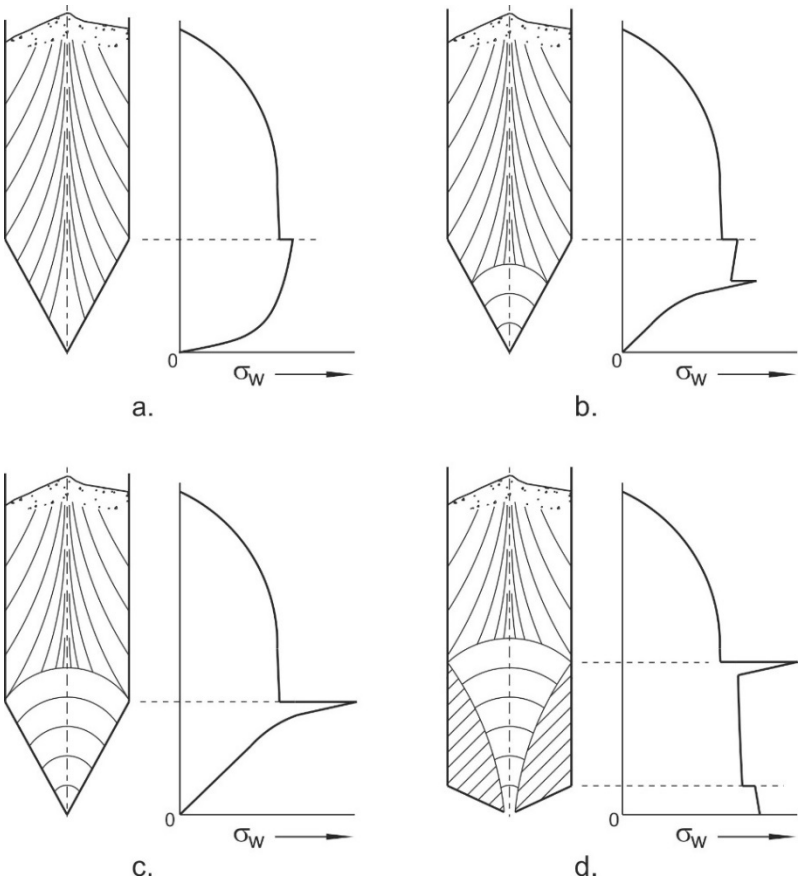

Fig. 3: Qualitative distributions of wall normal stresses, σ_w; the thin lines represent the assumed orientation of the major principal stress, σ_1 [2,3].

At the transition to the hopper, there is a discontinuity in the stress distribution. In the hopper, depending on its geometry and the bulk solid properties, the stress can continue to increase downwards, but also decrease (or initially increase and then decrease again). The stress state

that results after a silo has been filled is called the “active stress state” or “filling state”. As in the vertical part, in the active stress state the larger stresses in the hopper point in the vertical direction (major principal stress in the hopper axis is vertical).

When the bulk solid starts to be discharged, the entire bulk solid in a mass flow silo starts to move and the stress state in the hopper changes: Starting from the tip of the hopper, the so-called “passive stress state” is formed. The flow of the bulk solid through the convergent hopper causes the bulk solid to be compressed in the horizontal direction, while it is relieved in the vertical direction by flowing downward. Therefore, the greater stresses now act in the horizontal direction (greatest principal stress in the hopper axis is horizontal).

In Fig. 3b, which shows the state immediately after the start of emptying, the passive stress state is only present in the lower part of the hopper; in Fig. 3c (somewhat later than Fig. 3b) it is fully developed. This case is also referred to as the “emptying state”. In the vertical part of the silo, the active stress state is maintained, provided there are no local convergences (constrictions of the cross-section due to internals, bulges, etc.). At the transition from the active to the passive stress field (in the mass flow silo always at the transition between vertical section and hopper), which is referred to as a “switch”, a local stress peak occurs. If the bulk solid discharge is interrupted, the passive stress state is maintained in the hopper.

In a funnel flow silo, there are stagnant zones which are not moved during bulk solid is discharged. Therefore, the bulk solid only flows downwards within the flow zone that forms. If the flow zone meets the wall in the area of the silo shaft, as in Fig. 3.d, a transition from the silo shaft to a “hopper in the bulk solid” is formed there. Here, too, a stress peak occurs due to the convergent flow starting at this point. However, the position of the stress peak is unknown since the shape of the dead zone cannot be predicted.

While in Fig. 3 the normal stress on the hopper wall (wall normal stress, σ_w) was considered, Fig. 4 shows qualitatively the distribution of the vertical stress, σ_v, for the filling state (a) and the emptying state (b). The stress state in Fig. 4a corresponds to that in Fig. 3a (active), and that in Fig. 4b to that in Fig. 3c (passive). The distribution of the vertical stress, σ_v, in the hopper is similar to that of the wall normal stress, σ_w. In the filling state, the course of the vertical stress in the hopper depends on the surcharge load (vertical stress at the transition from the vertical section to the hopper), the bulk solid properties and the hopper geometry; the curve drawn in Fig. 4.a is to be regarded as a possible course. In the emptying state, the vertical stress decreases sharply towards the bottom, whereby the vertical stress in the lower hopper area is proportional to the distance to the imaginary hopper apex (“radial stress field”). The vertical stress at the outlet opening is independent of the stress acting at the upper end of the hopper in the emptying state (if the hopper is sufficiently high).

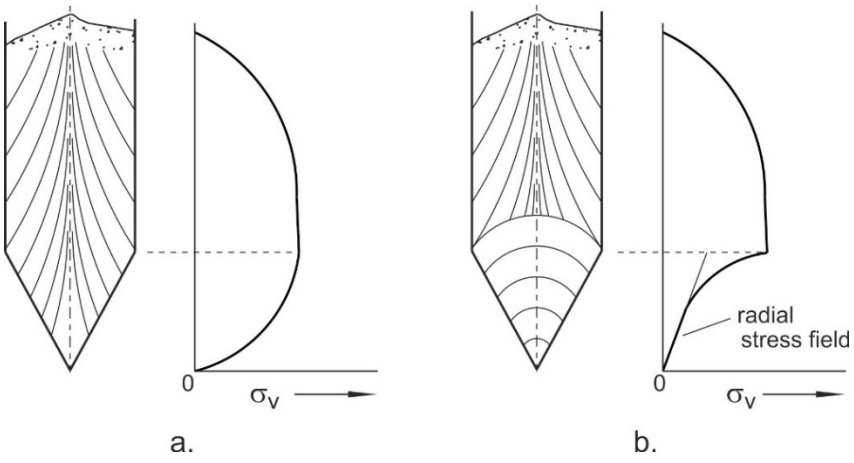

Fig. 4: Qualitative course of the vertical stress, σ_v, in the filling state (a) and in the emptying state (b) in a mass flow silo

Immediately after filling an empty silo (filling state, active stress state), the vertical stress at the outlet opening is greater than in the emptying state (passive stress state) [7-11]. In experiments, up to ten times greater vertical stresses were measured at the outlet opening in the filling state than in the emptying state [8, 9]. In Fig. 5 the filling and emptying of a silo and the related stresses are explained. The top diagram shows the filling level, h_f, versus time. As soon as bulk solid is discharged for the first time after the empty silo has been filled, the emptying condition is established, whereby the vertical stress, σ_v, at the outlet opening drops abruptly (Fig. 5, center). This means that after filling, the feeder must first be able to move the bulk solid under a large vertical stress, σ_v, which requires a large driving force, F_h (Fig. 5, bottom). As soon as the bulk solid has started to move, the emptying state with the lower vertical stress, σ_v (and thus smaller driving force, F_h) is established in the hopper within a short time.

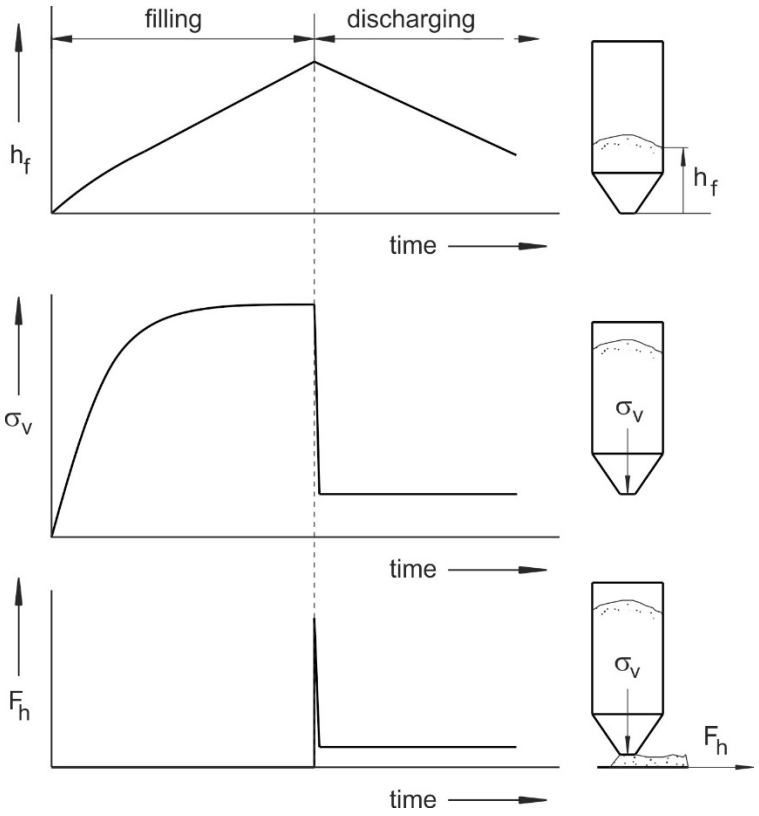

Fig. 5: Filling height, h_f, vertical stress at the outlet, σ_v, and feeder force, F_h, vs. time

4 Stress calculation

4.1 Calculation approaches (overview)

Three cases have to be considered for the calculation of stress distributions in silos:

- Stresses in the vertical section
- Stresses in the hopper (active stress state, filling state)
- Stresses in the hopper (passive stress state, emptying state)

Stresses in silos have been studied experimentally and theoretically since the end of the 19th century. After the stresses in the vertical section were initially considered (Janssen [12], Koenen [13]), this was later followed by work that also took into account the stress profile in the hopper.

The best known of these approaches are those of Jenike [7, 14], Walker [15, 16] and Walters [17, 18]. The first theoretical approaches were based on slice element methods, in which the equilibrium of forces on a slice element of infinitesimal thickness in the vertical section [12, 17] or in the hopper [15, 16, 18] was considered.

The calculation method developed by Jenike [7, 14] uses differential equations to describe the stresses that form in the hopper during discharge (emptying state or passive stress state). His calculation method also allows the design of silos by determining the hopper wall slope required for mass flow and the minimum dimensions of the outlet opening to avoid arching and ratholing. To facilitate the use of his method, Jenike presented the results of his calculations in the form of diagrams.

Among the later investigations, those of Enstad [19] and Benink [20] should be mentioned, who calculated the stresses in the hopper during discharge using slice element methods. For the calculation of the stresses in the filling state, the work of Motzkus [21] followed, among others, who recognized the assumptions of Walker and Walters as unrealistic and introduced improved assumptions.

Starting in the 1980s, the finite element method (FEM) was used for stress calculation (e.g. [22, 23]), but it did not become generally applied. Since the 1990s, DEM (discrete element method) simulations have been increasingly applied. Here, the bulk solid is not considered as a continuum, but the interactions between individual particles are simulated. This requires a high computational effort, so that still only limited numbers of particles can be simulated. Also, the complex shapes of the particles cannot yet be sufficiently approximated. Therefore, while DEM currently appears suitable for simulating simple processes in bulk solids (e.g. ball milling), it is not yet practically applicable for the stress calculations discussed in this section.

For practical calculations, therefore, in addition to the diagrams provided by Jenike, which are used to calculate the stresses in the hopper in the emptying state and for silo design for flow, the slice element methods have so far become established above all because of their relatively simple applicability. Thus, several standards for the determination of loads in silos, such as the current Eurocode [24], are based on Janssen's approach [12]. For the calculation of the stresses in the hopper in the filling state (active stress state), the slice element method of Motzkus gives useful results [9, 21], and for the emptying state, the relations derived by Enstad [19] are applicable.

Within the scope of this paper, the determination of stresses in the silo shaft is described according to the method derived by Janssen [12]. This method is also used in program Silo Stress Tool [25].

4.2 Calculation of the stresses in the vertical section of a silo

The stresses in the vertical section of a silo (active stress state) were calculated by Janssen [12] using a slice element method. He considered a volume element of infinitesimal height, *dz* (Fig. 6), which spans the entire silo cross-section. Assuming a constant vertical stress, σ_v, across the cross-section of the slice and a constant bulk density, ρ_b, a force equilibrium can be established at the slice element in the *z*-direction:

$$KA\sigma_v + g\rho_b A dz = A(\sigma_v + d\sigma_v) + \tau_w U dz \tag{2}$$

Introducing the wall friction angle,

$$\tan \varphi_x = \tau_w / \sigma_h \tag{3}$$

and the lateral stress ratio (see Eq (1)),

$$K = \sigma_h / \sigma_v \tag{4}$$

one obtains an ordinary differential equation for the vertical stress, σ_v.

$$\frac{d\sigma_v}{dz} + \sigma_v K \frac{U}{A} \tan \varphi_x = g \rho_b \tag{5}$$

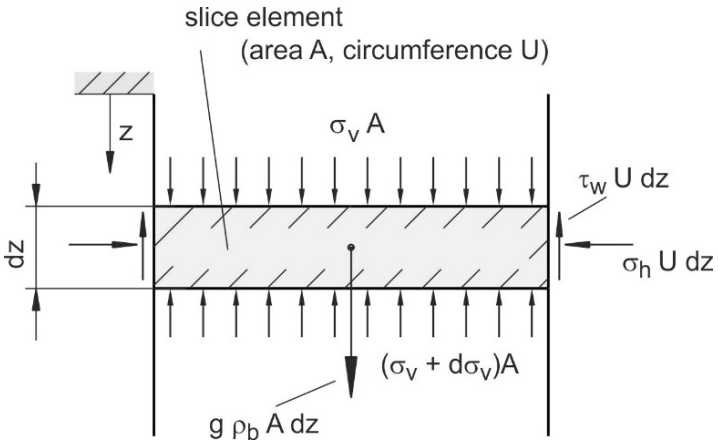

Fig. 6: Slice element in the vertical section

With the condition that a vertical surcharge stress, σ_{v0}, is acting on the top surface of the filling (at z=0), integration of the differential equation yields:

$$\sigma_v = \frac{g \rho_b A}{K \tan \varphi_x U} + \left[\sigma_{v0} - \frac{g \rho_b A}{K \tan \varphi_x U} \right] \cdot e^{\frac{-K \tan \varphi_x U z}{A}} \tag{6}$$

For the case σ_{v0} = 0, Eq. (6) yields the well-known "Janssen equation":

$$\sigma_v = \frac{g \rho_b A}{K \tan \varphi_x U} \left[1 - e^{\frac{-K \tan \varphi_x U z}{A}} \right] \tag{7}$$

Horizontal stress, σ_h, and wall shear stress, τ_w, follow from Eq. (6) by substituting K and tan φ_x, respectively, using Eqs. (3) and (4):

$$\sigma_h = \frac{g \rho_b A}{\tan \varphi_x U} \left[1 - e^{\frac{-K \tan \varphi_x U z}{A}} \right] + K \sigma_{v0} \cdot e^{\frac{-K \tan \varphi_x U z}{A}} \tag{8}$$

$$\tau_w = \frac{g \rho_b A}{U} \left[1 - e^{\frac{-K \tan \varphi_x U z}{A}} \right] + K \tan \varphi_x \, \sigma_{v0} \cdot e^{\frac{-K \tan \varphi_x U z}{A}} \tag{9}$$

For large values of z, the e-function in Eqs. (6) to (9) tends to zero. Thus, the final value $\sigma_{v\infty}$ of the vertical stress achievable for $z \to \infty$ is given by the expression in front of the brackets in Eq. (7):

$$\sigma_{v\infty} = \frac{g \rho_b A}{K \tan \varphi_x U} \tag{10}$$

The final value, $\sigma_{v\infty}$, is (for a sufficiently high silo) independent of the filling height. The surcharge stress, σ_{v0}, also has no influence on the final value, which can be easily understood from Eq. (6) (e-function approaches zero for large z). For bulk solids with "common" properties, the vertical stress is already quite close to the final value from a depth, z, equal to two to three times the cylinder diameter.

In addition to the bulk solid properties, the final value depends on the ratio A/U which is $A/U = d/4$ in a cylindrical silo (d = diameter of the cylindrical section). This means that the maximum possible stresses in the cylindrical section are proportional to the diameter, see Eqs. (6) to (10). For this reason, silos are usually built slim and tall, while tanks for storing liquids (e.g. oil tanks) are preferably built with small heights and large diameters because of the hydrostatic pressure.

The validity of Eq. (7) – the "Janssen equation" – has been proven in numerous experimental investigations, e.g. [5, 26, 27]. It is the basis of numerous standards for the calculation of stresses in silos (e.g. [24]).

To apply the Janssen equation, the bulk density, ρ_b, and the wall friction angle, φ_x, have to be known. Both can be measured with shear testers [1, 4]. The determination of the horizontal load ratio, K, is more difficult.

From experience, it is known that many bulk solids have a lateral stress ratio, K, between 0.3 and 0.6 (Section 2). Most of these stress ratios lie in the range of 0.4 to 0.5. Therefore, a value in this range would be useful for a rough estimate; in [7, 10] $K = 0.4$ is recommended.

For a rough calculation of the horizontal load ratio, an equation from soil mechanics proposed by Kézdi [28] is often used, which was given the factor 1.2 in the former German standard DIN 1055 Part 6 of 1987 [29]:

$$K = 1.2(1 - \sin \varphi) \tag{11}$$

φ is the angle of internal friction of the bulk solid. Often, the effective angle of internal friction, φ_e, resulting from a yield locus [1, 4] measured with a shear tester is used here, but this can lead to misestimations of the value of K [2, 3]. One step to gain more certainty in the determination is the recommendation in the current European standard [24] to measure the lateral stress ratio directly at uniaxial compression (Fig. 7). Measurements on an instrument built for this purpose, the "Lambdameter", show its applicability for determining the lateral stress ratio [2, 3].

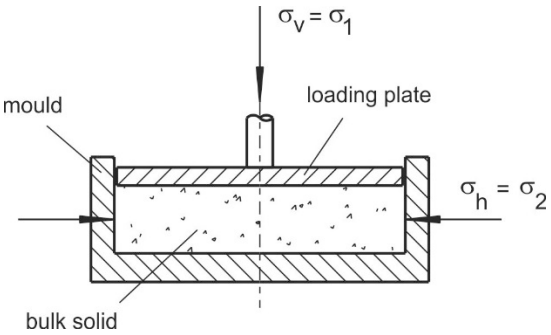

Fig. 7: Uniaxial compression with a "lambdameter"

4.3 Calculation of stresses in hoppers

The calculation of stresses in the hopper is too complex to be explained in detail here. Approaches as well as further literature references can be found in [1], with the program Silo Stress Tool [25] a simple solution for the estimation of stresses in the bulk solid is available.

A very rough estimation, which at least reflects the order of magnitude of the vertical stress at the outlet opening, σ_{va}, of a mass flow hopper in the emptying state, is possible with the following equations:

Conical hopper:

$$\sigma_{va} = 0.2 \cdot g \rho_b d \tag{12}$$

Wedge-shaped hopper:

$$\sigma_{va} = 0.4 \cdot g \rho_b b \tag{13}$$

d is the diameter of a circular outlet opening, b the width of an outlet slot, respectively, of the hopper. Depending on the type of feeder and the situation beneath the outlet opening of the hopper, the stresses due to the bulk solid beneath the hopper's outlet have to be added to the stresses calculated according to Eqs. (12) and (13) [1].

The stresses at the outlet opening in the filling condition depend on a number of influencing variables and cannot be calculated with simple equations. Experience from measurements (e.g. in [8, 9]) shows that the vertical stress in the filling condition, i.e. after filling of a previously empty silo, can be five to ten times as high as the vertical stress in the emptying condition (see Fig. 5).

5 Disturbances to the stress distribution

5.1 Switch

For the structural design of silos, the stresses acting on the silo walls must be known. On the one hand, these are the stresses explained in Sect. 3. On the other hand, there are additional stresses on the silo walls that arise, for example, from stresses that are uneven around the circumference or from local stress peaks.

In Sect. 3, reference was already made to the stress peak which forms in a mass flow silo during emptying at the transition from the vertical section to the hopper ("switch", Fig. 3c). In the following, the cause of the switch is explained (Fig. 8): The major principal stress, σ_1, in the axis of the vertical section acts in the vertical direction while the horizontal stress is the minor principal stress, σ_2 (active stress state). The principal stresses are represented in Fig. 8 by arrows whose length is a measure of the magnitude of the respective stress.

In the hopper, the bulk solid is compressed in the horizontal direction when flowing downward while it can expand in the vertical direction. This deformation of the bulk solid changes the directions of the principal stresses in that the horizontal stress becomes greater than the vertical stress. Thus, in the hopper axis, the minor principal stress, σ_2, acts in the vertical direction and the major principal stress, σ_1, acts in the horizontal direction.

For reasons of force equilibrium in the vertical direction, the vertical stress at the top of the hopper is equal to the vertical stress at the bottom of the vertical section. Therefore, the

horizontal stress in the hopper is much larger than the horizontal stress in the silo shaft. This explains the sudden increase in horizontal stress at the transition from the vertical section to the hopper.

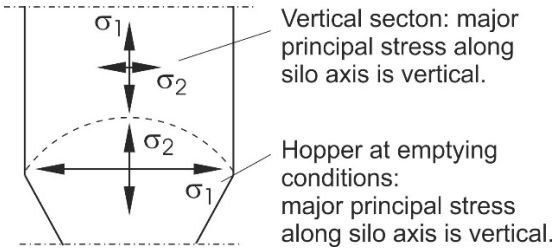

Fig. 8: Strress conditions at the transition

In mass flow silos, the "switch" occurs at the transition from the vertical section to the hopper. This must be taken into account in the structural design. In funnel flow silos, on the other hand, a stress peak occurs where the boundary line between the stagnant zone and the flowing bulk solid meets the silo wall (Fig. 3d). Thus, on the one hand, the stress peak is located in the more sensitive shaft area, and on the other hand, the (unpredictable) location of its occurrence varies over the circumference and also varies over time, so that the entire shaft area must be designed accordingly.

5.2 Imperfections

Even in the vertical section of a mass flow silo a local stress increase is possible. This effect is due to imperfections, i.e., local convergences and divergences, in the wall of the vertical section [1, 30, 31]. Imperfections can be caused by manufacturing inaccuracies, but also elements attached to the inner wall of the silo (ladders, temperature sensors, internals...).

Since a local reduction of the cross-section has a similar effect on the flow of bulk solids as a hopper, the passive stress state can be reached locally by an imperfection. Thus, the stress in the area of a local constriction of the cross-section can increase significantly since a similar effect occurs locally as at the transition from the vertical section to the hopper ("switch" due to the change of the orientation of the major principal stress). It can be assumed that the greater the imperfection in relation to the silo diameter and the less compressible the bulk solid, the stronger the effect.

5.3 Eccentric flow

If bulk solids flow downwards in the silo predominantly on one side, this is referred to as eccentric flow. The problem of eccentric flow – apart from the well-known disadvantages of funnel flow [1, 32] – is that the stress distribution over the circumference of the silo becomes uneven, which must be taken into account in the structural silo design.

To explain the effect, Figure 9a schematically shows the cross-section of a cylindrical part of a silo (diameter d) with an assumed flow zone (diameter d_f); Figure 9b shows a longitudinal section of the cylinder. The bulk solid flowing downward in the flow zone exerts downward shear stresses not only on the silo wall but also on the bulk solid at rest (stagnant zone), i.e., the flow zone is supported by shear stresses occurring at the silo wall and at the boundary to the bulk solid in the stagnant zone. The shear stresses are drawn as arrows in their direction of action. Thus, the flow zone can be considered as a "silo within the silo" with diameter d_f. From the equation describing the stresses in the cylindrical section (Eq.(7)), it is known that the maximum stresses achievable in a cylindrical section are proportional to its diameter. Therefore,

smaller stresses prevail in the flow zone than in the stagnant zone with the larger diameter $d > d_f$.

The lower stresses in the flow zone cause bending moments in the silo wall that would not occur with a uniform load. In the area of the flow zone, the wall becomes flatter (radius of curvature increases), which reduces its resistance to buckling in this area.

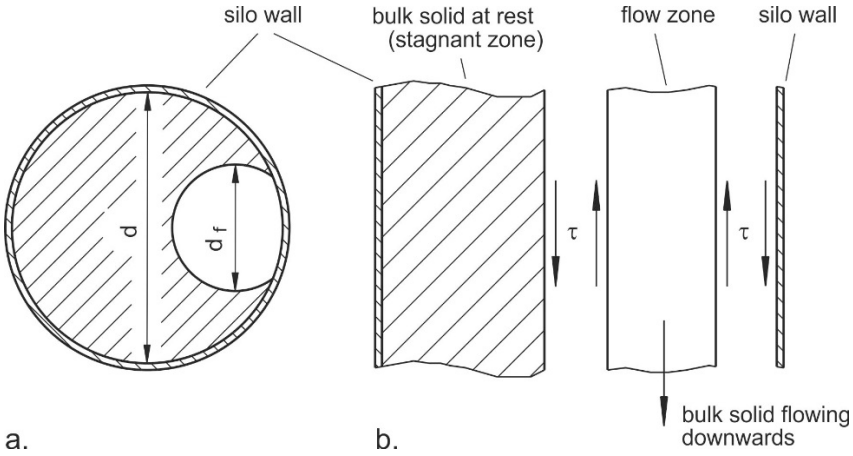

Fig. 9: Eccentric flow in the vertical section of a silo (schematic); a. top view; b. longitudinal section

Eccentric flow must be considered in the structural design of a silo. Therefore, the engineer doing the structural design must know how the bulk solid flows, e.g., how it is discharged.

Possible causes for eccentric flow are:

- Eccentrically arranged discharge opening or eccentrically arranged discharge device.
- Silo with a feeder or discharge device that discharges on one side only
- Silo with multiple outlet openings, not all of which are active.
- Funnel flow silo with asymmetrical flow zone
- Asymmetrical hopper

6 References

[1] Schulze, D.: Powders and Bulk Solids – Behavior, Characterization, Storage and Flow, 2nd ed., Springer (2021)

[2] Kwade, A. , Schulze, D., Schwedes, J.: Die direkte Messung des Horizontallastverhältnisses Teil 1 und 2, Beton- und Stahlbetonbau 89 (1994) 3, S. 58-63 und 89 (1994) 4, pp.117-119

[3] Kwade, A., Schulze, D., Schwedes, J.: Determination of the Stress Ratio in Uniaxial Compression Tests Part 1 and 2, Powder Handling & Processing 6 (1994) 1, S.61-65 und 6 (1994) 2, pp.199-203

[4] Schulze, D.: Flow properties of powders and bulk solids, https://www.dietmar-schulze.de/pdf/flowproperties.pdf

[5] Martens, P. (Hrsg.): Silohandbuch, Wilhelm Ernst&Sohn Verlag, Berlin, (1988)

[6] Arnold, P.C., McLean, A.G.: Improved analytical flow factors for mass-flow hoppers, Powder Technol. 15 (1976), pp. 279-281

[7] Jenike, A.W.: Storage and flow of solids, Bulletin No 123, Utah Eng. Exp. Station, Univ. of Utah, Salt Lake City, 1970

[8] Manjunath, K.S., Roberts, A.W.: Wall pressure-feeder load interactions in mass flow hopper/feeder combinations, bulk solids handling 6 (1986) 4, pp. 769-775 und 6 (1986) 5, pp. 903-911

[9] Schulze, D.: Untersuchungen zur gegenseitigen Beeinflussung von Silo und Austragorgan, Dissertation TU Braunschweig (1991) pdf
[10] Roberts, A.W.: Modern concepts in the design and engineering of bulk solids handling systems, TUNRA Ltd., The Univ. of Newcastle, N.S.W., Australien
[11] Arnold, P.C., McLean, A.G.: Bulk solids: Storage, flow and handling TUNRA Ltd., The 11Univ. of Newcastle, N.S.W., Roberts, A.W. Australien
[12] Janssen, H.A.: Getreidedruck in Silozellen, Z. Ver. Dt. Ing. 39 (1895), pp. 1045-1049
[13] Koenen, M.: Berechnung des Seiten- und Bodendrucks in Silozellen, Centralblatt der Bauverwaltung 16 (1896), pp. 446-449
[14] Jenike, A.W.: Gravity flow of bulk solids, Bulletin No 108, Utah Eng. Exp. Station, Univ. of Utah, Salt Lake City, 1961
[15] Walker, D.M.: An approximate theory for pressures and arching in hoppers, Chem. Eng. Sci. 21 (1966), pp. 975-997
[16] Walker, D.M.: A basis for bunker design, Powder Technology 1 (1967), pp. 228-236
[17] Walters, J.K.: A theoretical analysis of stresses in silos with vertical walls, Chem. Eng. Sci. 28 (1973), p. 13-21
[18] Walters, J.K.: A theoretical analysis of stresses in axially-symmetric hoppers and bunkers, Chem. Eng. Sci. 28 (1973), pp. 779-789
[19] Enstad, G.G.: A novel theory on the arching and doming in mass flow hoppers, Dissertation, Chr. Michelsen Inst., Bergen, Norwegen (1981)
[20] Benink, E.J.: Flow and stress analysis of cohesionless bulk materials in silos related to codes, Dissertation, Universität Twente, Enschede, Niederlande (1989)
[21] Motzkus, U.: Belastung von Siloböden und Auslauftrichtern durch körnige Schüttgüter, Dissertation TU Braunschweig (1974)
[22] Häußler, U.: Geschwindigkeits- und Spannungsfelder beim Entleeren von Silozellen, Dissertation Univ. Karlsruhe (1984)
[23] Rombach, G.: Schüttguteinwirkungen auf Silozellen - Exzentrische Entleerung, Dissertation Univ. Karlsruhe (1991)
[24] EN 1991-4 (2006): Eurocode 1: Actions on structures - Part 4: Silos and tanks (English)
[25] Schulze, D.: Silo Stress Tool (SSTOOL), program to assess stresses in containers and silos, Download at www.dietmar-schulze.de (2021)
[26] Hampe, E.: Silos, Band 1 (Grundlagen), VEB Verlag für Bauwesen, Berlin 1987
[27] Pieper, E., Wenzel, F.: Druckverhältnisse in Silozellen, Verlag Wilhelm Ernst & Sohn, Berlin 1964
[28] Kézdi, A.: Erddrucktheorien, Springer Verlag Berlin 1962
[29] DIN 1055 Teil 6: Lasten in Silozellen, Deutsche Norm (1987)
[30] Jenike, A.W., Johanson, J.R., Carson, J.W.: Bin loads - Part 2 and 3, Journ. of Eng. for Industry, Trans. ASME, Series B, Vol.95, No 1, Feb. 1973, pp.1-12
[31] Jenike, A.W.: Load Assumptions and distributions in silo design, Conf. on construction of concrete silos, Oslo, Norwegen, Januar 1977
[32] Schulze, D.: Storage of powders and bulk solids in silos, https://www.dietmar-schulze.de/pdf/storage.pdf